



Flow dynamics and size-based sorting of bidispersed colloidal particles in evaporating sessile water droplets: substrate heating and wettability effects

SURYANSH GUPTA¹, MAHESH R THOMBARE² and NAGESH D PATIL^{1,3,*}

¹Department of Mechanical Engineering, Indian Institute of Technology Bhilai, Bhilai 491001, India

²Department of Mechanical and Aerospace Engineering, Indian Institute of Technology Hyderabad, Hyderabad 502284, India

³Department of Bioscience & Biomedical Engineering, Indian Institute of Technology Bhilai, Bhilai 491001, India

e-mail: suryanshg@iitbhilai.ac.in; me22resch11012@iith.ac.in; nageshpatil@iitbhilai.ac.in

MS received 21 August 2023; revised 26 October 2023; accepted 1 November 2023

Abstract. The present work investigates the size based self-sorting behavior of particles near the contact line (CL) region of an evaporating sessile aqueous droplet containing bidispersed (1 and 3 μm) colloidal particles. Experiments were performed on hydrophilic glass and hydrophobic (Poly)dimethylsiloxane (PDMS) substrates maintained at different temperatures ($T_s = 23^\circ\text{C}$, 50°C , and 80°C). The role of substrate wettability and substrate temperature in the modulation of final deposition specifically, the self-sorting characteristics was examined. Various experimental techniques namely, high-speed visualization, 3D optical profilometry, fluorescence microscopy, and scanning electron microscopy were implemented to analyze the droplet evaporation and the morphology of the final deposition. As per the findings, in the case of hydrophilic substrate self-sorting existed at all temperatures. However, an appreciable improvement in the sorting quality was observed only at elevated temperatures. Particularly, for the case of $T_s = 80^\circ\text{C}$ in which the final deposition demonstrated better sorting of 1 and 3 μm particles. Since, most of the region in the CL's vicinity had a substantial reduction in the intermixing of 1 and 3 μm particles, thus effectively favouring the suppression of mixed region. In the case of nonheated ($T_s = 23^\circ\text{C}$) hydrophobic substrate it was observed that a continuous depinning of the CL, in conjunction, with a weak radial flow led to complete intermixing of the bidispersed particles thus, lacking any self-sorting behavior. However, for the heated hydrophobic substrate cases, a substantial delay in the depinning of the CL existed. This, in turn, combined with the outward-driven capillary flow and recirculatory thermal-Marangoni flow resulted in the manifestation of self-sorting phenomenon. This study is expected to offer novel fundamental insights into the underlying mechanisms that can be effectively leveraged, to gain better control of the governing parameters for the realization of desired sorting characteristics.

Keywords. Self-sorting; contact line; Marangoni flow; colloidal particles; PDMS; bidispersed particles.

1. Introduction

Sessile droplet evaporation is one of the most ubiquitous phenomena that constitute a plethora of different natural and manmade processes encountered in our daily lives. As it is omnipresent in most of the physical and biological processes spanning from, the everyday drying of a spilled sessile coffee droplet to, technologically advanced methods for medical diagnosis and forensic analysis based on the drying of blood droplets. However, owing to the extrinsic simplicity of a drying droplet it may rather appear to be a trivial process while, from a purely scientific perspective

the complexity involved is enormous. Such that, the research communities spread across multiple disciplines, are on a continuous quest to explore the multifaceted realm of droplet evaporation for almost the last three decades. Particularly, the evaporation of a droplet laden with colloidal particles has garnered a lot of scientific interest in the last two decades. This is also quite evident from the innumerable studies available in the literature that attempted to explore the different aspects related to the evaporating colloidal droplets, due to its potential applications in inkjet printing [1], coating [2], biomedicine [3], self-assembly [4], and many others. In the landmark work by Deegan [5], the scientific explanation to the emergence of a ring-like deposition from evaporating coffee droplets also, famously

*For correspondence

regarded as the “coffee-ring” (CR) effect was first reported. The findings underpinned the existence of a radially outward capillary flow that caused the advection of coffee particles towards the CL. Since then, extensive efforts have been directed towards the manipulation of the final deposit morphology, by controlling the various factors that either promote or inhibit the CR effect. Based on the literature [6], the different mechanisms responsible for the distribution of particles in the final deposition can be attributed to internal flows, evaporation kinetics, CL dynamics, evaporation modes and several others. These mechanisms are further governed by a host of different attributes such as colloidal particles (type, shape, size, and concentration), substrate wettability, interparticle and particle-substrate interactions, substrate temperature, and ambient conditions. In this context, to highlight the pivotal developments made so far for comprehending the influential role of the aforesaid factors, some of the notable works from the literature have been discussed next.

Bhardwaj *et al* [7] studied the evaporation of aqueous droplets containing titania nanoparticles on a glass substrate. Variation in the deposit morphology at different pH values of the droplets was explained by considering the DLVO interactions such as, Van der Waals and electrostatic forces. As per the observations, three types of colloidal deposition formed namely, uniform layer, central bump, and peripheral ring. Orejon *et al* [8] performed an experimental study to investigate the CL dynamics for water and ethanol droplets evaporating on hydrophobic substrates of different wettability. Further, titanium oxide nanoparticles were added to water in different quantities, and a comparison was made against the evaporation of pure water droplets on substrates of different hydrophobicity. It was observed that the stick-slip motion of the CL was related to the concentration of the nanoparticles. Chon *et al* [9] analysed the effect of variation in the size of nanoparticles (2, 11, 30, and 47 nm) on the morphology of final depositions. Their findings revealed that in the case of large-sized nanoparticles, coffee-ring patterns were formed. Whereas smaller nanoparticles led to a thicker uniform central deposition enclosed by a wide outer ring. Sommer *et al* [10] carried out an experimental study on the evaporation of droplets containing bidispersed nanoparticles (60 and 200 nm) on smooth substrate. As per the findings, the final deposition consisted of an ordered distribution of particles. Further, the self-assembly of larger particles lead to the formation of thick inner ring enclosed by an outer ring containing the particles in a hexagonal packing. Chhasatia and Sun [11] studied the effect of substrate wettability on the size-based sorting of particles near the CL. It was found that, increasing the substrate wettability led to an improvement in the size based separation of particles. This was attributed to the interplay of different forces (surface tension, drag force, particle-substrate interactions) and the extent of CL pinning existing during the different phases of evaporation. Yu *et al* [12]

investigated the deposit morphology obtained from the evaporating ethanol/water droplets containing large polystyrene microparticles on polymethylsiloxane (PDMS) surface. It was observed that at lower concentration the deposit pattern was characterized by a compact monolayer whereas, mountain-like deposition was obtained at higher concentration. Iqbal *et al* [13] conducted an experimental study on the evaporating droplets containing bidispersed colloidal particles on hydrophilic and hydrophobic substrates. A constitutive model was proposed to elucidate the effect of various forces responsible for the modulation of particle distribution in the final deposition. The model accounted for the different forces such as, surface tension force, Van der Waals and electrostatic forces, and drag force that acted on the particles. As per the findings in case of hydrophilic substrate, smaller particles (0.2 μm and 1.0 μm) moved to the pinned CL forming an outer ring, while the larger particles (3.0 μm and 6.0 μm) were dragged inwards to form an inner deposition. However, in the case of hydrophobic substrates the CL continuously depinned resulting in the formation of an inner deposition. All the studies mentioned so far were performed on nonheated substrates of different wettability. However, researchers in the recent years had also attempted to analyse the effect of substrate temperature on the evaporation dynamics, and ultimately on the final deposition. In this context, some of the studies pertaining to the effect of substrate temperature on the evaporating droplets containing colloidal particles are discussed below.

Li *et al* [14] examined the effect of substrate temperature on the evolution of dried deposits, obtained from the evaporating droplet containing colloidal suspensions on hydrophilic substrate. The findings revealed a gradual transition from the usual coffee ring pattern to a thin ring with a central stain. Moreover, it was also seen that the amount of central deposition augmented at elevated temperatures due to the enhancement in Marangoni recirculation. Parsa *et al* [15] analysed the morphologies of the final deposition obtained from, the evaporating aqueous nanofluid sessile droplets on smooth silicon substrate maintained at various temperatures (25°C to 99°C). Based on the substrate's temperature, three different deposit patterns emerged: a nearly uniform deposition, a dual ring pattern, and stick-slip pattern consisting of multiple rings. Patil *et al* [16] conducted experiments on the evaporating droplets containing monodispersed colloidal particles over glass and silicon substrates maintained at different temperatures. For nonheated hydrophilic substrate ring-like deposit patterns were observed however, for the case of a heated hydrophilic substrate a thin ring with an inner deposit formed. The thinning of the ring was attributed to the occurrence of stronger Marangoni recirculatory currents that, advected the particles away from the CL at elevated substrate temperatures. For the case of nonheated hydrophobic substrate an early onset of the CL depinning resulted in the formation of an inner deposition. On the contrary, substrate heating, in

conjunction, with a higher particle concentration favoured CL pinning thus, yielding a thin ring with inner deposit. Malla *et al* [17] performed experimental investigation to study the effect of non-uniformly heated glass substrate on evaporating aqueous droplets containing colloidal polystyrene particles. For droplets with smaller particles, the CL depinning on the hot side coupled with the asymmetric Marangoni recirculation caused a relatively higher advection of particles towards the cold side, thus giving rise to increased ring width on the cold side. Conversely, for larger particles the CL remained pinned along the hot side giving rise to a larger ring width along the hot side.

Based on the above literature survey it is evident that, substrate heating plays an influential role in dictating the evaporation dynamics that ultimately govern the final deposit morphology. Thus, there lies an opportunity to utilize substrate heating, for the modulation of size based self-sorting of particles from evaporating colloidal suspension droplets, as was first demonstrated in the study by Hendarto and Gianchandani [18]. Their observations clearly underscored the significance of substrate temperature variation ($T_s = 55\text{--}85^\circ\text{C}$), in the self-sorting of hollow glass particles (size ranging from 5 to 200 μm) from evaporating isopropyl alcohol droplets. Their findings revealed that due to Marangoni convection at higher temperatures, larger particles tend to migrate towards the droplet's interior to yield a central deposit. Simultaneously, smaller particles were found to advect towards the CL thus forming an outer ring. Moreover, they also reported that sorting of the particles improved at elevated temperatures. In the study by Patil *et al* [19], an experimental investigation on the evaporation of aqueous droplets containing mono- and bidispersed colloidal particles on heated silicon substrates was conducted. The coupled effects of particle size, size ratio, and substrate temperature on the CL dynamics and the self-sorting behaviour were examined. They reported a transition from no-sorting to sorting behaviour of particles at lower and higher temperatures, respectively. Moreover, a regime map was proposed based on the size ratio and the substrate temperature to demarcate the sorting and no sorting zones. Despite these investigations, for the case of hydrophilic substrate, such as glass, the effect of substrate temperature variation on the particle self-sorting characteristics is still not very well understood. Particularly, for the case where size of the particles is comparable or, the size ratio (size of smaller to larger particle) is not significant. Further, it is to be noted that due to pinning of the CL in glass substrates, sorting exists even under the ambient temperature. However, the quality of sorting, as determined by the relative size of the CL region occupied exclusively by the segregated particles, has not been analysed so far. Since, under the ambient temperature the CL region is also inhabited by an appreciable number of intermixed particles in the vicinity of the self-sorted particles. In view of these observations for the hydrophilic

substrates, it becomes indispensable to examine the role of substrate heating based modulation of the evaporation dynamics that will potentially aid in the improvement of self-sorting behaviour by either suppressing or, more favourably, eliminating the formation of mixed region near the CL.

On the other end, for surfaces with low wettability such as the hydrophobic substrates, most of the studies on the evaporating aqueous colloidal dispersion droplets have been performed on nonheated substrates [12, 13, 20, 21]. However, quite recently Gupta *et al* [22] performed an experimental investigation to study the effect of substrate temperature ($T_s = 22^\circ\text{C}$, 50°C , and 80°C) on the CL pinning-depinning dynamics of droplets containing mono-/bidispersed particles (3, 4.5 μm /3 and 4.5 μm) on hydrophobic PDMS. Their findings suggested that in the case of monodispersed colloidal droplets, a substantial delay in the depinning of CL prevailed at elevated temperatures. Whereas for the case of droplets containing bidispersed particles, a complete CL pinning was witnessed at $T_s = 80^\circ\text{C}$ thus, resulting in a distinctive ring-like deposit morphology. But despite the existence of a pinned CL, self-sorting of the bidispersed particles was not analysed in their study. To the best of our knowledge, there is hardly any study that investigated the self-sorting of particles for the evaporating bidispersed colloidal suspension droplets on nonheated/heated hydrophobic PDMS substrate. Therefore, this necessitates for a closer scrutiny on the feasibility of particle self-sorting behaviour facilitated by the substrate heating induced pinning of the CL for hydrophobic PDMS substrate. Since, it will have a strong bearing on the implementation of PDMS in the size based segregation of particles for potential applications such as, biosensors [23]. Based on this background, the motivation for the present work has been largely derived.

So, the overall objectives of the present study can be briefly summarised as follows:

- To experimentally investigate the self-sorting of particles near the CL for the bidispersed colloidal suspension (1 μm and 3 μm) droplets, on hydrophilic glass substrates maintained at different temperatures ($T_s = 23^\circ\text{C}$, 50°C , and 80°C).
- To analyse the variation in the particle sorting regimes obtained at different temperatures, and to ascertain the mechanism governing the underlying dynamics.
- To study the final deposition and the particle sorting behaviour for the evaporating droplets containing bidispersed colloidal dispersion on hydrophobic PDMS substrates maintained at different temperatures ($T_s = 23^\circ\text{C}$, 50°C , and 80°C).
- To analyse the morphology of the final deposition by varying the substrate temperature along with possible self-sorting behaviour of particles for the cases where, delayed depinning of the CL prevailed for a substantial duration.

2. Materials and methods

2.1 Preparation of colloidal solution, droplet generation, and substrate fabrication

The monodispersed colloidal dispersion containing fluorescent-polystyrene microsphere (PS) particles of diameter 1 and 3 μm (particle density as 1005 kg/m^3) with a particle concentration of 2.6% (wt./v) was purchased from Polysciences Inc. To obtain the solutions having a particle concentration of 0.05% (wt./v) and 0.1% (wt./v) (for the hydrophilic and hydrophobic experiments, respectively), the stock dispersions were diluted with deionized water in the required amount. Subsequently, equal proportions of both the as-prepared solutions were mixed to prepare the desired bidispersed colloidal solution containing 1 and 3 μm particles. Prior to conducting each experiment, we performed ultrasonication of the as-prepared solutions using the probe sonicator. The solutions were sonicated for an optimal duration of at least 30 minutes, which ensured uniform dispersion of the particles in the solution without any sedimentation or agglomeration. Note that the difference in the density of the PS particles and water is $\sim 5 \text{ kg/m}^3$, thus it can be considered as neutrally buoyant. This has been corroborated through the criterion given by Hamdi *et al* [24] for estimation of the non-dimensional Archimedes number (Ar). The Ar number express the effects of buoyancy or sedimentation given by the expression, $Ar = \frac{gd^3\rho_f(\rho_p-\rho_f)}{\rho_f}$, Where g is acceleration due to gravity, d is diameter of the particle, ρ_p is the density of the particles, and ρ_f is the density of the fluid. The condition for the tracer particles not affected, or only slightly affected by the phenomenon of sedimentation is $Ar < 5 \times 10^{-2}$. For our case we calculated the value of Ar number using the above expression and it was found to be $\sim 5 \times 10^{-7}$. This clearly indicates that sedimentation of the particles will be negligible. We also noted that the final deposition in our experiments had been primarily obtained by the advection of particles due to evaporation driven internal flows (Capillary and Marangoni flows). Lastly, the maximum evaporation time scale (t_{evp}) of the droplets was found to be in the order of $\sim 10^3 \text{ s}$. Whereas the order of magnitude of settling time for the largest particle size (3 μm) considered for our experiments was $\sim 10^5 \text{ s}$. This further validates the inconsequential role of particle sedimentation during the droplet evaporation.

For the experiments on hydrophilic substrates, glass slides (Sigma Aldrich Inc.) of size $75 \text{ mm} \times 2.5 \text{ mm}$ were utilized for the experiments. Whereas for the hydrophobic case, the substrates were fabricated in the laboratory by using the Polydimethylsiloxane (PDMS) polymer. For the fabrication process, first a 10:1 mixture of PDMS (Sylgard 184) and the curing agent was prepared in a glass petridish. After that, desiccation of the as-prepared mixture was performed in the vacuum chamber for 30 minutes to ensure

complete elimination of the entrapped gases. Then, the sample was cured inside a convection oven maintained at a temperature of 100°C for a period of two hours. Once the curing stage was completed, the sample was sized into square pieces of dimension $25 \text{ mm} \times 25 \text{ mm} \times 1.5 \text{ mm}$. Before the start of each experiment, cleaning of surfaces was performed sequentially using IPA and DI water, followed by complete drying on a hot plate at 60°C . Using the Advance Drop Shape Analyzer (Krüss Inc., Model: DSA25), the contact angle measurements were carried out for both the hydrophilic and the hydrophobic substrates by depositing a $1.5 \mu\text{L}$ volume droplet. As per the measurements performed on multiple locations over the substrate, the static equilibrium contact angle for the glass and the PDMS substrates were found to be $35 \pm 2^\circ$ and $108 \pm 8^\circ$, respectively. For the experiments, droplets of volume $1.5 \pm 0.3 \mu\text{L}$ were dispensed on the PDMS substrate using a variable volume micropipette (range: $0.2\text{--}2.0 \mu\text{L}$ and volume resolution: $0.01 \mu\text{L}$). To ensure gentle deposition of the microlitre sized droplets, we dispensed the droplets using a micropipette held in the closest proximity to the substrate. This allowed the droplets to be deposited on the substrate with minimum initial velocity to prevent any undesirable oscillations after deposition. Finally, we recorded the droplet evaporation only after any unwanted droplet's interfacial oscillations (if any) settled down.

2.2 Experimental setup

The experimental arrangement is shown in the figure 1, which involves a high-speed camera (Model: Phantom VEO-1330 series), working distance of Lens (Qioptiq Inc.): 9.5 cm , pixel resolution: $11 \pm 0.2 \mu\text{m}/\text{pixel}$) for the side visualization of evaporating droplets, screw-controlled levelling platform, horizontal linear stage, and a closed chamber for isolation. For heating the substrates to the desired temperatures, a thermoelectric heating module (TEC Inc.) was used, and the operating power was supplied using a multi-range DC power supply (Gw INSTEK Inc.). For the background illumination during side visualization, an adjustable intensity white LED light source (12V , 30 Watts) was used. It is to be noted that for all the experiments the recording was carried out at 50 frames per second.

Post processing of the recorded videos was performed using the ImageJ software for image processing. A MATLAB code [25] was implemented on the extracted images for the acquisition of droplet related parameters by analysing the pixel information from the instantaneous images. While carrying out the experiments, the surrounding air temperature and relative humidity were $22 \pm 3^\circ\text{C}$ and $50 \pm 5\%$, respectively. To ensure the repeatability of results, each experiment was performed at least thrice. The final deposition was imaged at $5\times$ magnification using a fluorescent microscope (Olympus IX73). Visualisation of

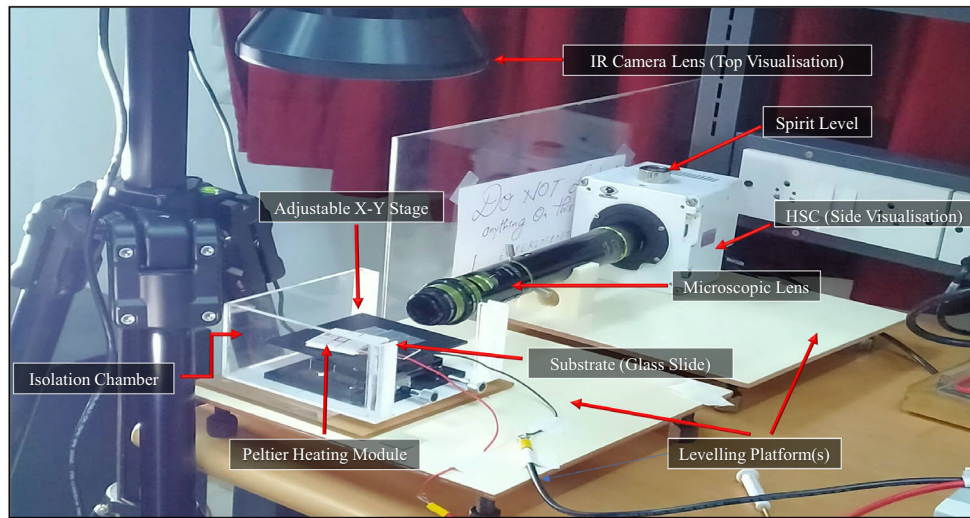


Figure 1. Image representing the experimental setup used in the study of droplet evaporating on substrates of different wettability.

the particle arrangement near the contact line was performed at a magnification of $2500\times$ using the scanning electron microscope (Carl Zeiss Inc.). For the contact line profile characterization of the final deposit patterns, 3D optical profilometer (S neox, SENSO FAR Inc.) was utilized. The ring profile measurements were performed at multiple azimuthal locations and the average values were calculated.

3. Results and discussions

3.1 Evaporation of bidispersed colloidal suspension droplets on hydrophilic glass maintained at different substrate temperatures

The images of the transient variation of evaporating droplets acquired using the high-speed camera have been illustrated in the figure 2a–c. To analyse the qualitative variation, the normalised droplet related parameters viz. wetted diameter (d_w^*), contact angle (θ^*), and volume (v^*) are plotted against the normalised time (t^*) as shown in the figure 2d. It can be observed from the variation of d_w^* that, at all temperatures a constant contact radius (CCR) [26] mode of evaporation prevailed for a substantial duration of the droplet’s lifetime. However, during the end stages a mixed mode [27] is observed in which the droplet’s wetted diameter and contact angle exhibit a drastic reduction until complete evaporation. The final deposit morphology obtained for the hydrophilic glass substrates at $T_s = 23^\circ\text{C}$, 50°C , and 80°C have been depicted in the figure 3a–c. It is observed that due to CCR mode of evaporation, a ring-like morphology is witnessed for both the nonheated ($T_s = 23^\circ\text{C}$) and heated ($T_s = 50^\circ\text{C}$ and 80°C) substrates. Interestingly, these observations are consistent with the findings

reported by Malla *et al* [28] for a similar range of particle sizes and concentration of evaporating colloidal suspension droplets on nonheated hydrophilic substrate. For a quantitative estimation of the deposit patterns, profile characterization of the outer ring near the CL has been performed as shown in the figure 4a. It is found that at all substrate

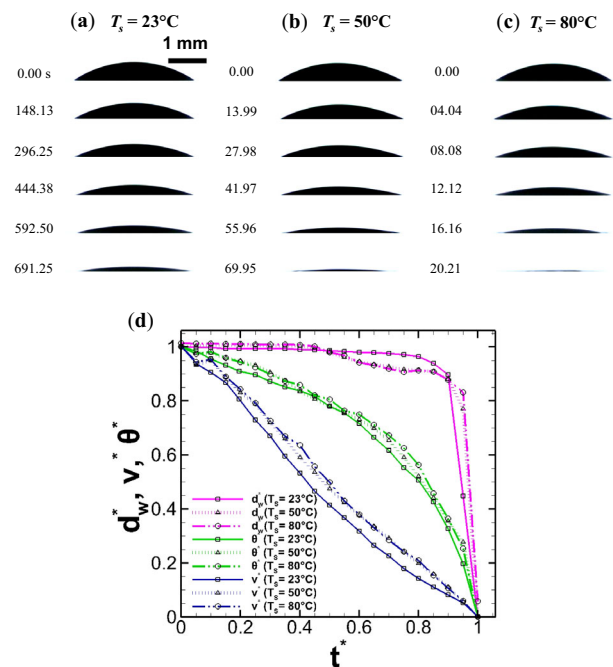


Figure 2. Side visualization depicting the transient evolution of evaporating colloidal droplets on glass substrate maintained at different temperatures, (a) $T_s = 23^\circ\text{C}$ (b) $T_s = 50^\circ\text{C}$ and (c) $T_s = 80^\circ\text{C}$. (d) Plot illustrating the variation of normalised droplet related parameters with respect to normalised time.

temperatures, a uniform monolayer having a width of $\sim 30 \mu\text{m}$ forms on the ring wherein, the maximum height of the outer ring is almost equal to the largest particle size ($d_p = 3 \mu\text{m}$). To investigate the variation in the arrangement of particles near the CL at different substrate temperatures, SEM characterization of the final depositions is performed. As shown in the figure 3d–e, the images correspond to the arrangement of 1 and 3 μm particles lying in the vicinity of the CL region. As per the observations, one of the distinctive features common at all temperatures is the existence of self-sorting behaviour leading to the segregation of particles on the outermost region of the CL. However, there lies characteristic differences in the morphology of the particle distribution at different temperatures. To ascertain the characteristic differences in morphology, the CL has been classified into various distinct regions as shown in the figure 3d. It can be observed that the outer periphery of the CL is almost entirely inhabited by 1 μm particles, followed by a depletion region (which is devoid of any particles), and thus facilitate in the clear demarcation

of the zones corresponding to 1 and 3 μm particles. Although the third zone majorly consists of the 3 μm particles but, their undisturbed presence is limited only till the first row. Since, in all the subsequent rows lying towards the droplet's center, 1 μm particles are found to be interspersed along with the 3 μm particles giving rise to a mixed zone. As a result, the number density of the self-sorted 3 μm particles is significantly affected vis a vis 1 μm particles. For $T_s = 50^\circ\text{C}$, the morphology of the particle arrangement is similar to the previous case as shown in the figure 3e, with the only exception being a considerable reduction in the size of the depletion region. However, at $T_s = 80^\circ\text{C}$ there is a dramatic reduction in the number of 1 μm particles interspersed in the mixed zone as shown in the figure 3f. This makes the mixed zone virtually non-existent, due to the absence of 1 μm particles in majority of the regions located along the CL. Thus, inevitably resulting in a zone largely comprising of the 3 μm particles. The rationale behind the observed variations in the self-sorting characteristics at different temperatures can be elucidated based

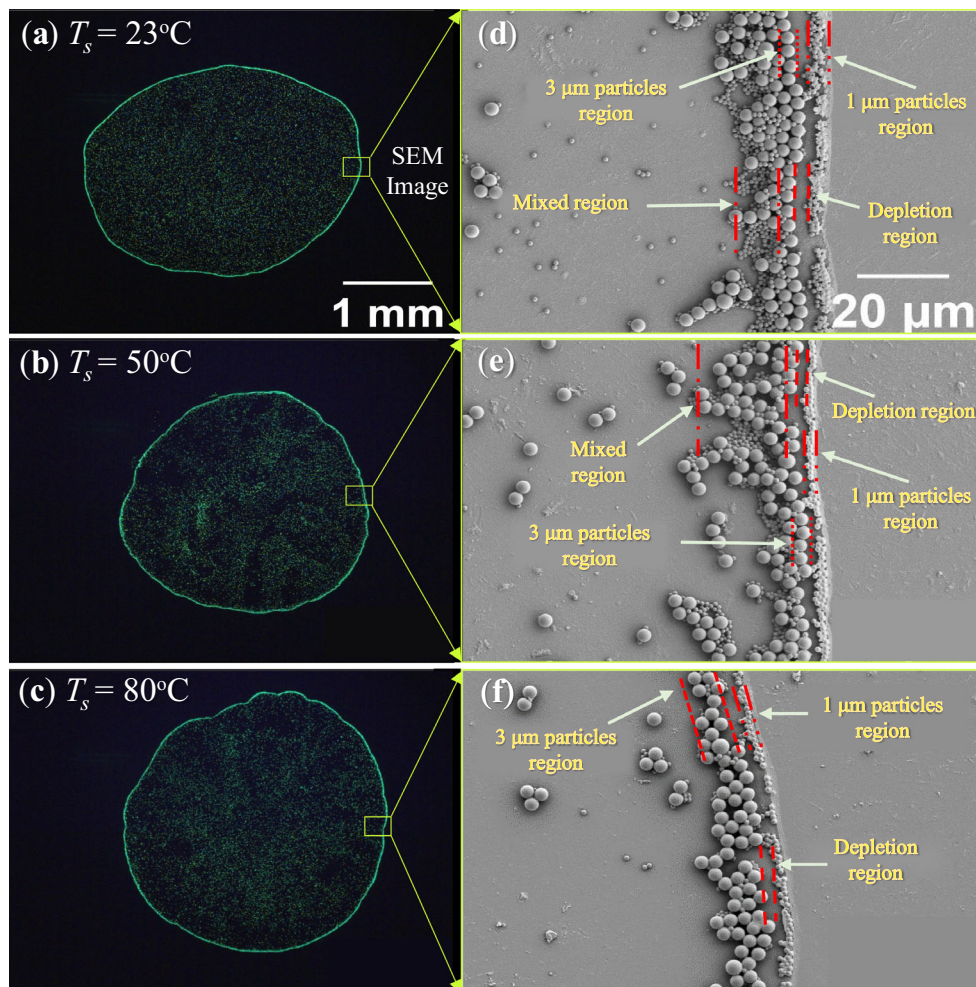


Figure 3. Fluorescent (a–c) and SEM (d–f) images of the deposit morphologies obtained from the evaporation of droplets containing bi-dispersed polystyrene fluorescent particles of diameter 1 μm and 3 μm on glass substrate at different substrate temperatures.

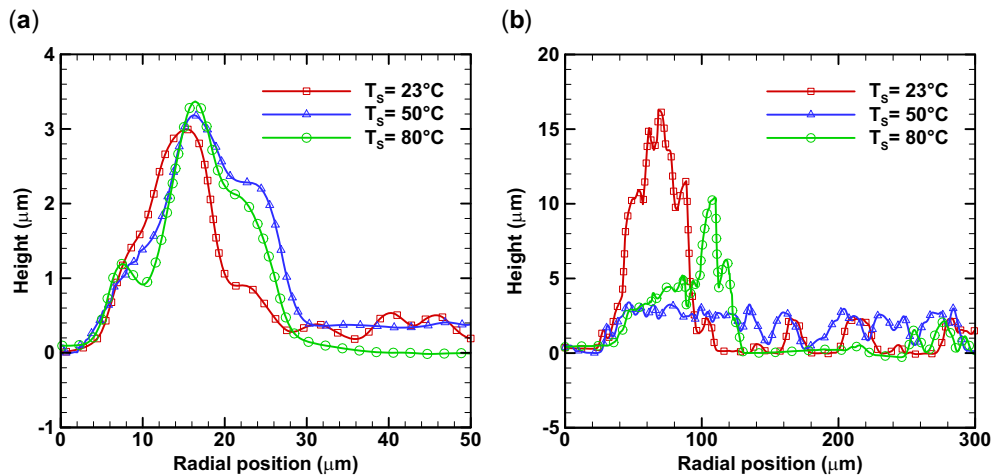


Figure 4. Graph representing the ring profile variation with respect to the radial location at different substrate temperatures for (a) hydrophilic and (b) hydrophobic substrates.

on the internal flow dynamics. For a better visual understanding, we have presented a schematic as shown in the figure 5 illustrating the distinctive differences in the flow patterns, and the corresponding particle deposition near the CL for $T_s = 23^\circ\text{C}$ and 80°C . For the nonheated hydrophilic substrate ($T_s = 23^\circ\text{C}$), owing to the contact line singularity strong capillary flows emerge that advect majority of the particles towards the CL [29]. As the particles approach the CL, they encounter a gradual reduction in the size of the droplet's meniscus such that, the advected particles are constrained as per their relative sizes [30]. Consequently, there exists a size based segregation of the particles near the CL wherein, the $1\ \mu\text{m}$ particles invariably occupy the outermost region followed by the $3\ \mu\text{m}$ particles. However, due to a concurrent influx of the bidispersed particles towards the CL, the region containing the self-sorted $3\ \mu\text{m}$ particles is affected by the invasion of $1\ \mu\text{m}$ particles as noted earlier.

For $T_s = 50^\circ\text{C}$ and $T_s = 80^\circ\text{C}$ (as shown in figure 5b), due to substrate heating a surface tension gradient is generated across the vapor-liquid interface [16]. As a result, a circulatory thermal Marangoni convection is established which is directed from the CL towards the apex [16]. The presence of these currents significantly impacts the arrangement of particles migrating towards the CL. Since, the combined effects of the Marangoni and the radial flow inevitably determines the morphology of the final deposition. As mentioned earlier for the nonheated substrate case, most of the particles are transported towards the CL due to the capillary flows. However, for heated cases the existence of Marangoni convection causes a greater number of bidispersed particles (except for those deposited in the stagnation zone) to be carried away from the CL towards the droplet's interior [29]. It must also be noted that the extent of this effect become more prominent at elevated substrate temperatures leading to stronger circulations [16]. Evidently at $T_s = 80^\circ\text{C}$, there exists an

appreciable decrease in the number of bidispersed particles at the CL as compared to the other cases. But interestingly, this decrease is found to be relatively higher in the case of $1\ \mu\text{m}$ particles vis a vis $3\ \mu\text{m}$ particles. Especially in the mixed region, there is a drastic reduction in the number of $1\ \mu\text{m}$ particles that finally give rise to a region largely dominated by the $3\ \mu\text{m}$ particles (as shown in the figure 3f). This, in effect, greatly enhance the self-sorting characteristics by substantially retarding the formation of the mixed region along the CL.

3.2 Evaporation of bidispersed colloidal suspension droplets on hydrophobic PDMS substrates maintained at different substrate temperatures

The transient variation of the evaporating colloidal suspension droplets acquired using the high-speed camera have been depicted in the figure 6a–c. For the qualitative analysis of the evaporation process, normalised droplet related parameters viz. wetted diameter (d_w^*), contact angle (θ^*), and volume (v^*) are plotted against the normalised time (t^*) as shown in the figure 5d. For the case of nonheated hydrophobic substrate, the contact angle initially reduces until the receding angle is reached at $t^* \sim 0.15$. Thereafter, the depinning of the CL begins and the evaporation proceeds in constant contact angle (CCA) mode. This trend is also evident in the figure 6b which shows a monotonic decrease in the d_w^* with respect to t^* at $T_s = 23^\circ\text{C}$. However, for the case of heated hydrophobic substrates ($T_s = 50^\circ\text{C}$ and 80°C), there is an appreciable delay in the depinning of the CL since, the evaporation proceeds in the CCR mode for a substantial duration until $t^* \sim 45\%$. Notably, these observations corroborate well with the findings reported in the study by Gupta *et al* [22], which underscored the influential role of

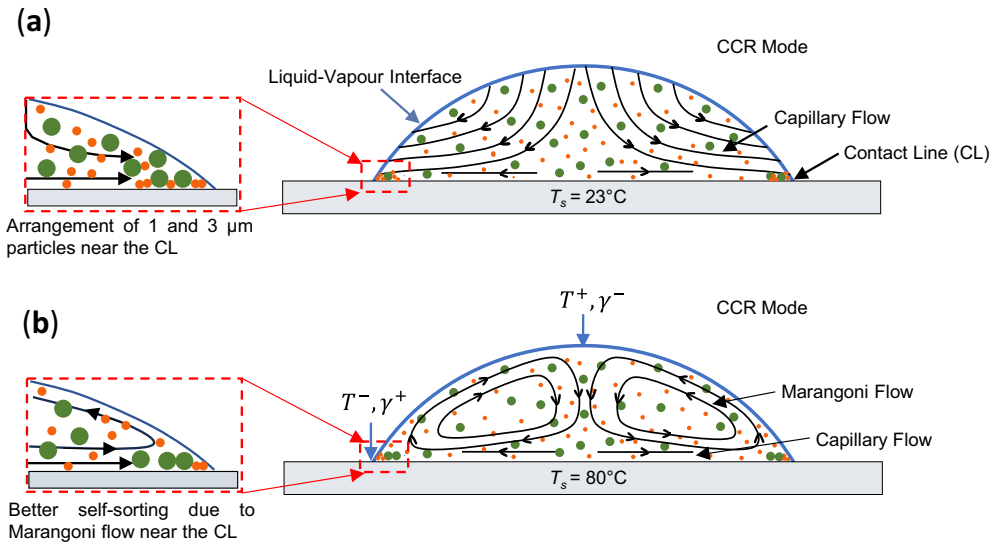


Figure 5. Schematic depiction of the internal flow pattern inside the evaporating droplets containing bidispersed particles (1 and 3 μm) and the self-sorting characteristics near the CL on hydrophilic glass maintained at (a) $T_s = 23^\circ\text{C}$ and (b) $T_s = 80^\circ\text{C}$. Here, T^+ and T^- denotes the higher and lower liquid-vapor interfacial temperature at the apex and CL, respectively and γ^+ and γ^- corresponds to the higher and lower values of surface tension at those locations.

substrate heating on the CL pinning-depinning dynamics. The reason for the variation in the evaporation dynamics due to substrate heating is attributed to, the combined role of the pinning force exerted by the bidispersed particles on the CL, and the coupled effects of the thermal Marangoni circulations and outward driven capillary flows [22, 31, 32]. Interestingly, even after the onset of CL depinning, the overall change in the wetted diameter is considerably lower for the heated cases as compared to

the nonheated case. This can also be verified from the final depositions depicted in the figure 6–c which show an appreciable difference in their respective sizes. Regarding the deposit morphology, a ring-like inner deposit is manifested at all substrate temperatures ($T_s = 23^\circ\text{C}$, 50°C and 80°C), with the smallest ring diameter of ~ 1 mm obtained in the case of $T_s = 23^\circ\text{C}$. Whereas, for the case of heated substrates the ring diameter is almost identical (1.33 mm and 1.28 mm at $T_s = 50^\circ\text{C}$ and 80°C ,

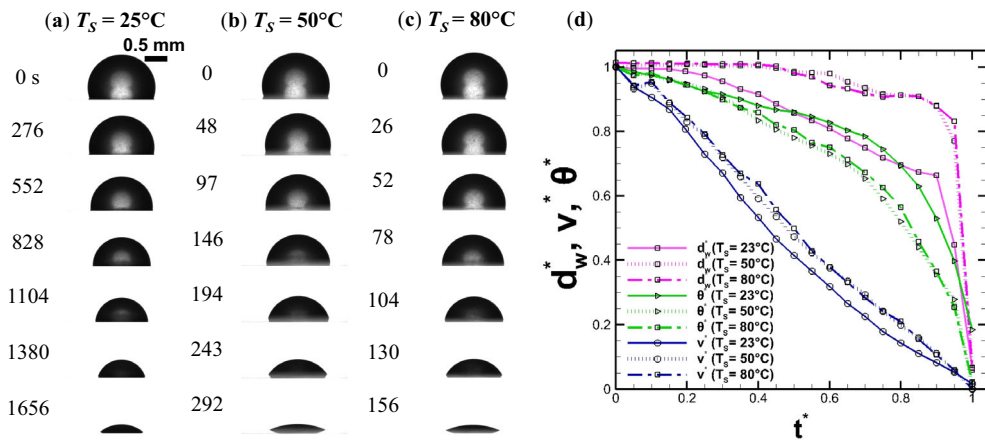


Figure 6. Side visualization depicting the transient evolution of evaporating droplets on hydrophobic PDMS substrate maintained at different temperatures, (a) $T_s = 23^\circ\text{C}$ (b) $T_s = 50^\circ\text{C}$ and (c) $T_s = 80^\circ\text{C}$ (d) Plot illustrating the variation of normalized droplet related parameters with respect to normalized time.

respectively), but the ring width is different and is higher for the deposition formed at $T_s = 50^\circ\text{C}$. For the quantitative estimation of the distribution of particles lying on the inner ring, profile characterisation has been performed. As shown in the figure 4b, due to the formation of a multilayered deposition a ridge-like feature is observed in the case of $T_s = 23^\circ\text{C}$ and 80°C . The height ($\sim 11 \mu\text{m}$) of the ridge is maximum in the case of nonheated substrate but, the width is observed to be slightly higher in the case of heated substrate. However, for the case $T_s = 50^\circ\text{C}$ the bidispersed particles are found to be deposited in the form of a uniform monolayer on the inner ring. To further examine the organization of these particles on the inner ring, SEM characterisation of the depositions obtained at different temperatures has been performed. As per the observations, there are distinctive differences perse in the arrangement of particles as shown in the figure 7. To understand the underlying mechanism a schematic has been illustrated in the figure 8 elucidating the transient evolution of the evaporating droplets for the heated and nonheated ($T_s = 23^\circ\text{C}$) and nonheated cases ($T_s = 80^\circ\text{C}$). It is to be noted that for the case of non-heated substrate, the flow pattern depicted in figure 8a is only a gross representation of the internal flow field based on the findings reported in the literature [33]. For $T_s = 23^\circ\text{C}$ as shown in the Figure 8a, it is found that both the 1 and 3 μm particles are intermixed across the entire CL. This is due to the occurrence of CL depinning prevalent during CCA mode of evaporation, resulting in the dragging of particles as the CL is mobilised. So the moving CL completely destabilizes the arrangement of particles in the zones that may have otherwise displayed self-sorting, if any. On the contrary, for the heated cases ($T_s = 50^\circ\text{C}$ and 80°C) self-sorting of the 1 μm particles prevailed on the peripheral ring. As shown in the figure 7d, e, there exists a well-defined depletion region and a row of self-sorted 3 μm particles along the CL. In terms of the sorting quality, it is observed that at $T_s = 50^\circ\text{C}$ there is a discontinuity in the arrangement of the 1 μm particles on the outer region besides a lack of any appreciable self-sorting of the 3 μm particles. However, at $T_s = 80^\circ\text{C}$ deposition is characterized by a continuous ring of segregated 1 and 3 μm particles with a well-defined separation facilitated by the depletion region. In essence, transition from no-sorting to sorting by substrate heating and improvement in the sorting characteristics by elevating the temperature has been clearly demonstrated in our findings. Finally, it can be inferred that substrate heating plays an influential role in the modulation of deposition morphology and ultimately, on the self-sorting characteristics of colloidal suspension droplets evaporating on hydrophobic and hydrophilic substrates.

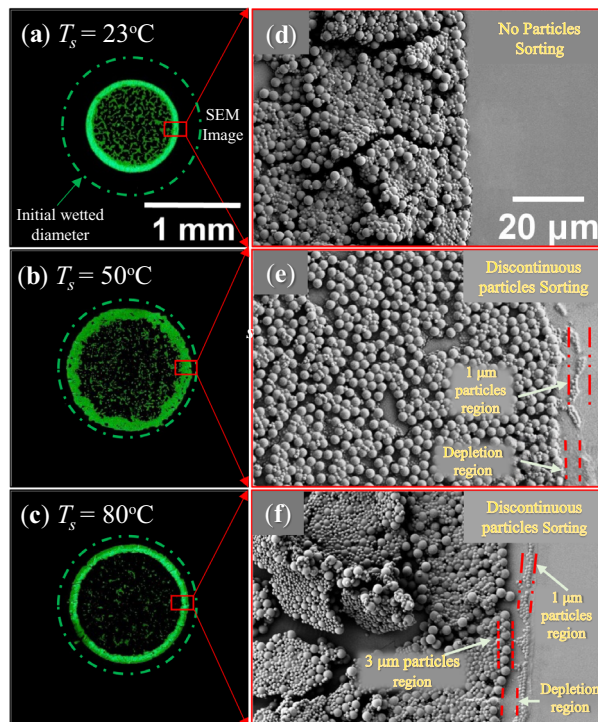


Figure 7. Fluorescent (a–c) and SEM (d–f) images of the deposit morphologies obtained from the evaporation of droplets containing bi-dispersed polystyrene fluorescent particles of diameter 1 μm and 3 μm on PDMS substrate at different substrate temperatures.

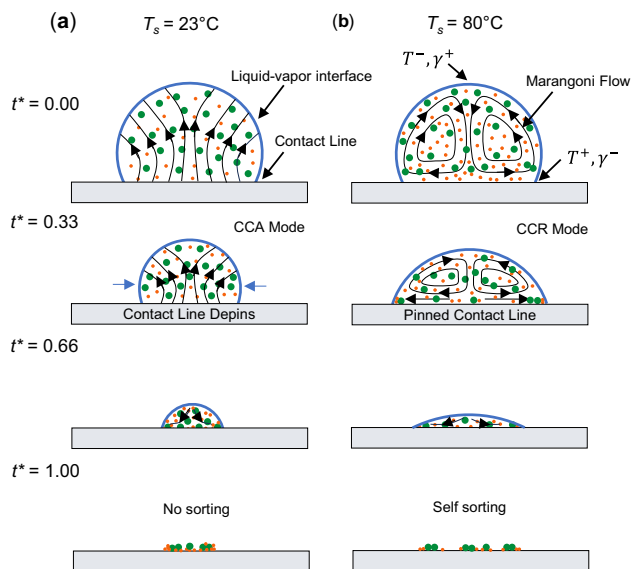


Figure 8. Schematic for the temporal evolution of evaporating droplets with liquid flow patterns and the sorting characteristics on hydrophobic PDMS substrates maintained at a temperature of (a) $T_s = 23^\circ\text{C}$ and (b) $T_s = 80^\circ\text{C}$. It is to be noted that t^* denotes the normalised evaporation time.

4. Conclusions

We investigated the effect of substrate temperature on the self-sorting of particles for an evaporating sessile water droplets containing bidispersed (1 and 3 μm) colloidal particles on hydrophilic glass and hydrophobic PDMS substrates. The salient findings of this study can be summarised as follows:

- In the case of hydrophilic substrate, the evaporating colloidal suspension droplets followed CCR mode at all substrate temperatures. Based on the arrangement of particles in the final depositions, the CL region is classified as, self-sorted 1 and 3 μm particles region, depletion region, and mixed region. The sorting characteristics are found to improve at elevated substrate temperature. Specifically, at $T_s = 80^\circ\text{C}$ a complete sorting of the 1 and 3 μm particles is manifested with an apparent elimination of the mixed region.
- The underlying cause for the enhancement in the self-sorting behaviour is ascribed to the presence of thermal Marangoni circulatory flows for the heated substrates. These convective currents advect the particles from the CL region towards the droplet's interior. This, in turn, reduces the effective number of the smaller particles deposited near the CL (at $T_s = 80^\circ\text{C}$), and improves the sorting quality through an almost complete suppression of the mixed region.
- For the case of nonheated hydrophobic substrates ($T_s = 23^\circ\text{C}$), the colloidal suspension droplets follow CCA mode of evaporation for a majority of the droplet's lifetime. As a result, a continuous depinning of the CL prevails, which simultaneously drag the particles along with it to yield an inner ring-like deposition.
- For the case of heated hydrophobic substrate ($T_s = 50^\circ\text{C}$ and 80°C), the colloidal suspension droplets undergo CCR mode of evaporation due to the delayed depinning of the CL. As a result, self-sorting of the 1 μm particles is obtained in the vicinity of the inner ring, together with the formation of the depletion and mixed regions towards the ring's interior. As far as the sorting quality is concerned, a discontinuous and continuous ring of particles is observed for the inner depositions obtained at $T_s = 50^\circ\text{C}$ and $T_s = 80^\circ\text{C}$, respectively.
- The delay in the depinning of the CL is attributed to the increased resistance offered to the CL motion in presence of the bidispersed particles, in conjunction with the coupled effects of the capillary and Marangoni flows. Therefore, this results in the self-sorting of the bidispersed particles along the outermost portion of the inner ring-like depositions.

Abbreviations

CL	Contact line
PDMS	Polydimethylsiloxane
PS	Polystyrene microsphere
CCR	Constant contact radius
SEM	Scanning electron microscopy

List of symbols

d_w^*	Normalised wetted diameter
v^*	Normalised volume
t^*	Normalised evaporation time
T_s	Substrate temperature
$^\circ\text{C}$	Degree Celsius
θ^*	Normalised contact angle
γ	Liquid-vapour surface tension

Acknowledgements

N.D.P. acknowledges the financial support from Indian Institute of Technology Bhilai, under the research initiation grant (IIT Bhilai/D/2506, Project code 2006900), to develop experimental setup used in the present work. N.D.P. also acknowledges the financial support from the Science and Engineering Research Board (SERB), Department of Science and Technology, Government of India, New Delhi, by the grant number SRG/2020/001947. All the authors are thankful to the Central Instrumentation Facility (CIF), IIT Bhilai, for providing access to scanning electron microscope (SEM) for imaging.

Data availability The data that support the findings of this study are available from the corresponding author upon reasonable request.

Declarations

Conflict of interest The authors have no conflict of interest to disclose. All the authors have contributed equally.

References

- [1] De Gans B J, Duineveld P C and Schubert U S 2004 Inkjet printing of polymers: state of the art and future developments. *Adv. Mater.* 16: 203–213.
- [2] Kim H, Boulogne F, Um E, Jacobi I, Button E and Stone H A 2016 Controlled uniform coating from the interplay of Marangoni flows and surface-adsorbed macromolecules. *Phys. Rev. Lett.* 116: 124501
- [3] Sefiane K 2010 On the formation of regular patterns from drying droplets and their potential use for bio-medical applications. *J. Bionic Eng.* 7: S82–93
- [4] Bigioni T P, Lin X-M, Nguyen T T, Corwin E I, Witten T A and Jaeger H M 2006 Kinetically driven self-assembly of highly ordered nanoparticle monolayers. *Nat. Mater.* 5: 265–270

- [5] Deegan R D 2000 Pattern formation in drying drops. *Phys. Rev. E* 61: 475–485
- [6] Patil N D and Bhardwaj R 2019 Recent developments on colloidal deposits obtained by evaporation of sessile droplets on a solid surface. *J. Indian Inst. Sci.* 99: 143–156
- [7] Bhardwaj R, Fang X, Somasundaran P and Attinger D 2010 Self-assembly of colloidal particles from evaporating droplets: role of DLVO interactions and proposition of a phase diagram. *Langmuir* 26: 7833–7842
- [8] Orejon D, Sefiane K and Shanahan M E R 2011 Stick-slip of evaporating droplets: Substrate hydrophobicity and nanoparticle concentration. *Langmuir* 27: 12834–12843
- [9] Choi Y, Han J and Kim C 2011 Pattern formation in drying of particle-laden sessile drops of polymer solutions on solid substrates. *Korean J. Chem. Eng.* 28: 2130–2136
- [10] Sommer A P, Ben-Moshe M and Magdassi S 2004 Size-discriminative self-assembly of nanospheres in evaporating drops. *J. Phys. Chem. B* 108: 8–10
- [11] Chhasatia V H and Sun Y 2011 Interaction of bi-dispersed particles with contact line in an evaporating colloidal drop. *Soft Matter* 7: 10135–10143
- [12] Yu Y S, Wang M C and Huang X 2017 Evaporative deposition of polystyrene microparticles on PDMS surface. *Sci. Rep.* 7: 14118
- [13] Iqbal R, Majhy B, Shen A Q and Sen A K 2018 Evaporation and morphological patterns of bi-dispersed colloidal droplets on hydrophilic and hydrophobic surfaces. *Soft Matter* 14: 9901–9909
- [14] Li Y, Lv C, Li Z, Quéré D and Zheng Q 2015 From coffee rings to coffee eyes. *Soft Matter* 11: 4669–4673
- [15] Parsa M, Harmand S, Sefiane K, Bigerelle M and Deltombe R 2015 Effect of substrate temperature on pattern formation of nanoparticles from volatile drops. *Langmuir* 31: 3354–3367
- [16] Patil N D, Bange P G, Bhardwaj R and Sharma A 2016 Effects of substrate heating and wettability on evaporation dynamics and deposition patterns for a sessile water droplet containing colloidal particles. *Langmuir* 32: 11958–11972
- [17] Malla L K, Bhardwaj R and Neild A 2020 Colloidal deposit of an evaporating sessile droplet on a non-uniformly heated substrate. *Colloids Surf. A Physicochem. Eng. Asp.* 584: 124009
- [18] Hendaro E and Gianchandani Y B 2013 Size sorting of floating spheres based on Marangoni forces in evaporating droplets. *J. Micromech. Microeng.* 23: 075016
- [19] Patil N D, Bhardwaj R and Sharma A 2018 Self-sorting of bidispersed colloidal particles near contact line of an evaporating sessile droplet. *Langmuir* 34: 12058–12070
- [20] Yu Y-S, Xia X-L, Zheng X, Huang X and Zhou J-Z 2017 Quasi-static motion of microparticles at the depinning contact line of an evaporating droplet on PDMS surface. *Sci. China Phys. Mech. Astron.* 60: 094612
- [21] Uno K, Hayashi K, Hayashi T, Ito K and Kitano H 1998 Particle adsorption in evaporating droplets of polymer latex dispersions on hydrophilic and hydrophobic surfaces. *Colloid. Polym. Sci.* 276: 810–815
- [22] Gupta S, Thombare M R and Patil N D 2023 Pinning and depinning dynamics of an evaporating sessile droplet containing mono- and bidispersed colloidal particles on a nonheated/heated hydrophobic substrate. *Langmuir* 39: 3102–3117
- [23] Bowman E K, Wagner J M, Yuan S-F, Deaner M, Palmer C M, D’Oelsnitz S, Cordova L, Li X, Craig F F and Alper H S 2021 Sorting for secreted molecule production using a biosensor-in-microdroplet approach. *Proc. Natl. Acad. Sci.* 118: e2106818118
- [24] Hamdi M, Havet M, Rouaud O and Tarlet D 2014 Comparison of different tracers for PIV measurements in EHD airflow. *Exp. Fluids* 55: 1702
- [25] Dash A, Bange P G, Patil N D and Bhardwaj R 2020 An image processing method to measure droplet impact and evaporation on a solid surface. *Sādhanā* 45: 287
- [26] Kadhim M A, Kapur N, Summers J L and Thompson H 2019 Experimental and theoretical investigation of droplet evaporation on heated hydrophilic and hydrophobic surfaces. *Langmuir* 35: 6256–6266
- [27] Gunjan M R and Raj R 2017 Dynamic roughness ratio-based framework for modelling mixed mode of droplet evaporation. *Langmuir* 33: 7191–7201
- [28] Malla L K, Bhardwaj R and Neild A 2019 Analysis of profile and morphology of colloidal deposits obtained from evaporating sessile droplets. *Colloids Surf. A Physicochem. Eng. Asp.* 567: 150–160
- [29] Gelderblom H, Diddens C and Marin A 2022 Evaporation-driven liquid flow in sessile droplets. *Soft Matter* 18: 8535–8553
- [30] Parsa M, Harmand S, Sefiane K, Bigerelle M and Deltombe R 2017 Effect of substrate temperature on pattern formation of bidispersed particles from volatile drops. *J. Phys. Chem. B* 121: 11002–11017
- [31] Josyula T, Mahapatra P S and Pattamatta A 2022 Internal flow in evaporating water drops: dominance of Marangoni flow. *Exp. Fluids* 63: 49
- [32] Josyula T, Wang Z, Askounis A, Orejon D, Harish S, Takata Y, Mahapatra P S and Pattamatta A 2018 Evaporation kinetics of pure water drops: thermal patterns, Marangoni flow, and interfacial temperature difference. *Phys. Rev. E* 98: 52804
- [33] Bhardwaj R 2018 Analysis of an evaporating sessile droplet on a non-wetted surface. *Colloid Interface Sci. Commun.* 24: 49–53

Springer Nature or its licensor (e.g. a society or other partner) holds exclusive rights to this article under a publishing agreement with the author(s) or other rightsholder(s); author self-archiving of the accepted manuscript version of this article is solely governed by the terms of such publishing agreement and applicable law.